Adsorption of Methylene Blue (MB) Dye Using NiO-SiO_2NPs Synthesized from Aqueous Solutions: Optimization, Kinetic and Equilibrium Studies

Davoudi, Shahnaz*[+]

Department of Chemistry Omidiyeh Branch, Islamic Azad University, Omidiyeh, I.R. IRAN

ABSTRACT: *The applicability of the synthesized NiO-SiO_2NPs as a novel adsorbent for eliminating Methylene Blue (MB) dye from aqueous media was investigated. Various techniques including BET, FT-IR, XRD, SEM, and EDS were used to characterize this novel adsorbent. The investigation showed the applicability of NiO-SiO_2NPs as an available, suitable, and low-cost adsorbent for the proper removal of MB dye from aqueous media. The effect of pH, adsorbent dosage (dose), initial MB dye concentration (C_0) contact time (tc), and temperature (T) on the removal percentage (Ad%) of MB dye onto NiO-SiO_2NPs was studied and the optimum value of each factor was determined (pH=7, dose=0.1g, C_0=30 mg/L, tc=15 min, and T=298.0 K). The experimental equilibrium data were fitted to the conventional isotherm models and accordingly, Langmuir isotherm has good applicability for the explanation of experimental data with maximum adsorption capacity of the MB dye for SiO_2 and NiO-SiO_2NPs were roughly 117.0 and 140.0 mg/g respectively. Kinetics experiments were performed to investigate the adsorption kinetics, the pseudo-second-order kinetics coincided quite with the kinetic results. The thermodynamic behavior of the adsorption process was studied by considering the effect of temperature on the adsorption capacity, where the results showed that the process is spontaneous ($\Delta G^0_{ad} < 0$) at the used temperature range and exothermic ($\Delta H_{ad}^0 < 0$) with $\Delta S^0_{ad} < 0$. Based on the magnitude of $\Delta H^0_{ad} < 0$, it was concluded that the studied adsorption process is a physisorption one.*

KEYWORDS: *Methylene Blue (MB); Adsorption capacity; Removal percentage; Kinetics; Thermodynamics.*

INTRODUCTION

The severity of water pollution has resulted from the economic development adopted by humans overall in the world. Textile industries consume huge quantities of water and generate an enormous amount of impurities including dyes, detergents, additives, suspended solids, aldehydes, heavy metals, non-biodegradable matter, and insoluble substances [1]. It was estimated that greater than 80,000 t of reactive dyes are manufactured and subsequently utilized yearly, and this enables the reader to assume the extent of pollution caused by these dye groups [2]. Wastewaters in industries like textile, paper, rubber, plastic, leather, cosmetic, food, and drug industries contain

***** *To whom correspondence should be addressed.*
+ *E-mail: sdavoudi632@gmail.com*
1021-9986/2022/7/2343-2357 *15/$/6.05*

dyes and pigments which are hazardous and can cause allergic dermatitis, skin irritation, cancer, and mutation in living organisms [1-3]. Also, inhalation of them can affect the respiratory tract with symptoms of rapid or difficult breathing, while mouth ingestion can affect the gastrointestinal tract with symptoms of burning sensation, nausea, vomiting, hyperhidrosis disorder, cognitive impairment disorder, micturition disorder, and methemoglobinemia–like syndromes [4]. Because of their synthetic nature and complex aromatic molecular structures, dyes are almost non-biodegradable in the ecosystem. The importance of the potential pollution of dyes and their intermediates has been incited by the toxic nature of many dyes, different mutagenic effects, skin diseases, and skin irritation and allergies. Moreover, they are dangerous because their microbial degradation compounds, such as benzidine or other aromatic compounds have a carcinogenic effect [5]. The existence of the dyes in water, even at very low dosages, is extremely undesirable. Methylene blue ($C_{16}H_{18}ClN_3S$, MB) a well-known cationic dye, is used in various industries as a coloring agent and redox indicator widely used by industries [6]. At dosages exceeding 5 mg/Kg, MB may precipitate serious serotonin toxicity and serotonin syndrome. Some of the by-far known side effects of MB are mild bladder irritation, dizziness, headache, sweating, nausea/vomiting, diarrhea, frequent urination, or stomach cramps. Lots of methods have been investigated and applied for the removal of the hazardous dyes from wastewater [7]. Therefore, the removal of dyes before their discharge into aquatic systems is required to safeguard human and ecosystem health. Various treatment methods have been utilized for the removal of dyes from contaminated wastewater, including advanced oxidation processes, catalytic degradation, adsorption, and electrochemical degradation. Among these methods, adsorption is a promising approach owing to its simple operational design, non-susceptibility to pollutants, reusability, high efficiency, low cost, and relatively low waste production [8,9].

The adsorption method is especially suitable for solving dyes, environmental, gases, and metals problems and has many advantages, so it has become the focus and hot spot of research. Adsorption is one of the best and simple techniques for the removal of toxic and noxious impurities in comparison to other conventional protocols such as flocculation, membrane filtration, advanced oxidation, ozonation, photocatalytic degradation, and biodegradation [10-12]. The physical and chemical properties of an adsorbent determine the effectiveness of an adsorption process extremely. The valuable properties are considered as follows: having high adsorption capacity, being available and recoverable, and also being economical. In recent years, it was tried to eliminate specified organics from water samples by applying diverse potential adsorbents. In this connection, Magnetic NanoParticles (MNPs) as unique adsorbents thanks to their small diffusion resistance, high adsorption capacity, and large surface areas have extensively been noticed. Their application for instance, in the separation of chemical species like dyes, environmental pollutants, gases, and metals has proven to be successful [13-15]. Several adsorbents such as oxides (nickel oxide, manganese oxide, titanium dioxide, iron oxides, aluminum oxide, zirconium oxide, mixed oxides, etc.), agricultural and industrial wastes, biosorbents and Activated Carbon (AC) have been tested by different researchers for the removal of dyes from aqueous solution [16-19]. Activated carbon is a commonly used adsorbent, but its price is expensive and regeneration is difficult. Therefore, preparing SiO_2NPs as an alternative to exorbitant or noxious adsorbents for the elimination of ions from wastewater attracted our attention [20,21]. With controllable porosity, surface area and high available adsorption sites of $Ni(OH)_2$ and NiO nanocomposites enhance its utility for various other [22].

In the present study, after synthesizing NiO-SiO_2NPs as a unique adsorbent, its characterization was performed by using Fourier Transform InfraRed (FT-IR) spectroscopy, Scanning Electron Microscopy (SEM), and X-Ray Diffraction (XRD). In the process of MB dye removal, the effects of important variables such as contact time, pH of the solution, adsorbent dosage, temperature, and MB dye initial concentration as well as the dye removal percentage as a response were investigated and optimized [23,24]. The pseudo-second-order rate equation matched quite the adsorption kinetics of MB dye adsorption and it was very evident. Also, the Langmuir isotherm model could be better for the related results than other models and explain better the adsorption equilibrium data. However, specific isotherm models such as Freundlich, Langmuir, and Temkin were used to fitting the experimental equilibrium data. Moreover, it was shown that the kinetics

of the adsorption process was more favorable with the pseudo-second-order equation than the pseudo-first-order or diffusion model equations. As a final result, the capability and usefulness of SiO_2 and NiO-SiO_2NPs for removing the MB dye from aqueous media were effectively proven.

EXPERIMENTAL SECTION

Reagents and materials

All chemicals used are commercially available and used as received. Polyethylene glycol (PEG) (Molecular weight 35,0 g/mol) and octadecyl tri methyl ammonium bromide (CTAB) were purchased from Sigma-Aldrich. Tetra ethoxy silane (TEOS) was purchased from Alfa Assar. Nitric acid (69%), ammonia (28–30%), nickel nitrate hexahydrate ($Ni(NO_3)_2.6H_2O$) Methylene Blue dye, chemicals were supplied from Merck (Darmstadt, Germany), All used chemicals were of reagent grade and utilized without further purification. For the pH adjustment, hydrochloric acid (HCl_{aq}) and sodium hydroxide ($NaOH_{aq}$) were applied.

Instrumentation

UV–vis spectrophotometer (Jasco, Model UV–Vis V-530, Japan). Fourier Transform InfraRed (FT-IR) spectra was from PerkinElmer (FT-IR spectrometer BX, Germany). The morphology of samples was studied by scanning electron microscopy (SEM: KYKY-EM 3200, Hitachi Company, China) under an acceleration voltage of 26kV). The pH/Ion meter (model-728, Metrohm Company, Switzerland, Swiss) was used for the pH measurements. Laboratory glassware was kept overnight in 10% nitric acid solution.

Synthesis of mesoporous silica nanoparticles

MSNs were synthesized by modified Stober's method using cetyl trimethyl ammonium bromide (CTAB, 99%, Spectrochem) as surfactant material and tetraethyl orthosilicate (TEOS, 98%, Kemphasol) as a precursor for SiO_2 [25]. In a typical synthesis, 100 mg of CTAB was dissolved in 25 mL water-ethanol mixture (4:1) and an appropriate amount of ammonia solution (NH_4OH, 25%, Merck) was added to the CTAB solution under continuous magnetic stirring. Then 1 mL of TEOS was added dropwise and the temperature of the solution was maintained at 50 °C for 4 h. The obtained product was dried overnight at 60 °C, after washing with ethanol and mille water following centrifugation (6000 rpm for 10 min).

Synthesis of NiO-SiO_2 nanoparticles

NiO-SiO_2 nanoparticles were synthesized *via* the non-casting method. Nickel nitrate hex hydrate (3.1 M) solution was impregnated into as prepared silica nanoparticles after degassing them under a vacuum. The wet nanoparticles were heated at 150°C for 10 h (1°C/min). The impregnation process was repeated at least five times to get uniform NiO-SiO_2 nanoparticles. Later, synthesized nanoparticles were calcined at 400°C for 5 h at a rate of 1 °C/min [26].

A typical adsorption experiment

Generally, the batch method is currently used in adsorption studies [27]. This method includes the following steps: (I) selecting an adequate solution of adsorbate with a known initial concentration in a suitable (e.g., 50.0 mL, C_0=30.0 mg/L). (II) Adding an adequate dosage of adsorbent to the previous solution (e.g., 0.10 g). (III) Adjusting pH and temperature on desirable values (e.g., 7.0 and 25.0 °C). (IV) Stirring the resultant mixture in step III for a suitable contact time (e.g., 15.0 min). (V) Separating the solid phase from the solution phase under the equilibrium state by an effective technique (e.g., centrifuge). (VI) The MB dye concentration in the solution was measured using a double beam UV–Vis spectrophotometer (Jasco, Model UV–Vis V-530, Japan), set at wavelengths 675 nm for MB dye. (VII) Evaluating the removal percentage (Ad%) and adsorption capacity of the adsorbent (q_e) from the following equations:

$$\%\ \text{Ad dye} = \frac{(C_0 - C_t)}{C_0} \times 100 \quad (1)$$

C_0 and C_t refer to the initial concentration of dye (mg/L) and the concentration of dye at any time (mg/L) respectively.

$$q_e = \frac{(C_o - C_e)V}{W} \quad (2)$$

In the above equation, q_e, C_0, C_c, V, and W refer to adsorption capacity (mg/g), the primary concentrations of dye (mg/mL), the equilibrium concentrations of dye (mg/mL), the volume of the aqueous phase (mL), and the weight of the adsorbent (g), respectively [28].

RESULTS AND DISCUSSION

Characterization of adsorbent

BET analysis of NiO-SiO_2NPs

Fig. 1. The pore structure parameters of molecular sieve materials such as N_2 adsorption-desorption

Table 1: Characteristics of the SiO_2 and NiO-SiO_2NPs.

Parameter	pH	Bulk density (g/mL)	Surface area (m^2/g)	Particle size range (µm)	Loss of mass on ignition
Value	7.0	0.607	250.0	45.0-250.0	0.6235

isothermal curve and specific surface area were determined by a micrometric ASAP2010M adsorption analyzer. The sample was dropped onto the slide for conducting layer treatment, at 77 K liquid nitrogen temperature and the operating voltage was 20 KV. The specific surface area was calculated using the Brunner-Emmett-Teller (BET) method. Bulk density, surface area, and loss of mass on ignition are shown in Table 1. The bulk density affects the rate of adsorption of MB dye solution by NiO-SiO_2NPs. In the present study, the bulk density was less than 1.0 indicating and hence enhancing the adsorption of MB dye from an aqueous solution [29]. The surface area of NiO-SiO_2NPs in the present research study was (45.231 m^2/g and 1.34×10^{-2} cm^3/g).

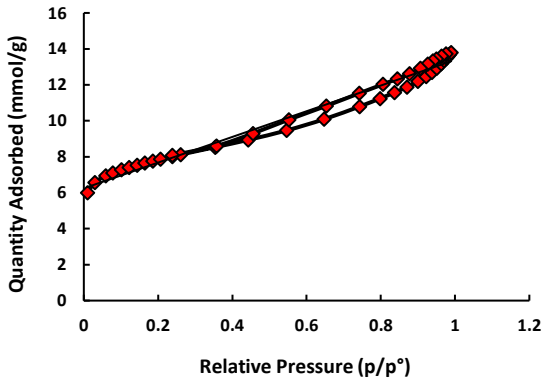

Fig. 1: N_2adsorption–desorption isotherms of NiO-SiO_2NPs.

FT-IR analysis

The characteristic functional groups of NiO-SiO_2NPs, NiONPs, and SiO_2 were investigated using FTIR spectra (Fig. 2). A peak appeared around 492 cm^{-1} corresponds to the stretching mode of Ni–O bonds in the spectra of NiONPs and NiO-SiO_2NPs. The broad band around 3427 cm^{-1} was assigned to the symmetric and asymmetric O–H stretching vibrations of water present in NiONPs and/or AC functional groups. The peak appeared at ~1086 cm^{-1} and 792 cm^{-1} stretching of asymmetric Si-O-Si and symmetric Si-O-Si, respectively. In other words, the observed peaks in the range of 400-4000 cm^{-1} are probably attributed to the absorbed water molecules in the KBr matrix or the prepared nanostructures or their probable interaction [30].

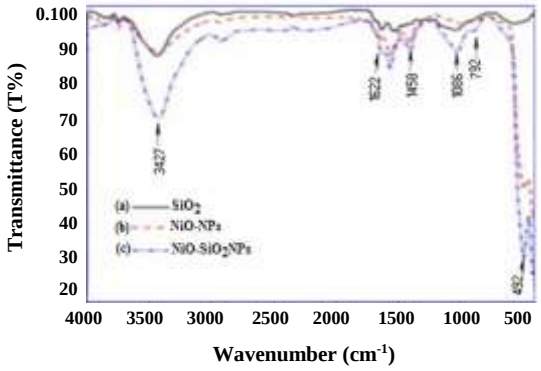

Fig. 2: (a) FT-IR spectrum of SiO_2 (b) NiO-NPs and (c) NiO-SiO_2NPs.

XRD analysis

Different X-ray emission peaks are NiO-SiO_2NPs, the adsorption of (MB) dye, based on Fig. 3, show peaks at 2θ= 30.5°, 36.8°, 46.2°, 53.6°, and 64.2° belonging to the lattice planes of (100), (101), (102), (110) and (103), confirm the cubic structure of NiO-SiO_2NPs [31]. However, the great intensity of the signal at 36.8° (101) confirmed that there is a slight amount of amorphous state material. Indeed, the perfect synthesis of NiO-SiO_2NPs can be judged by looking at XRD pattern of it.

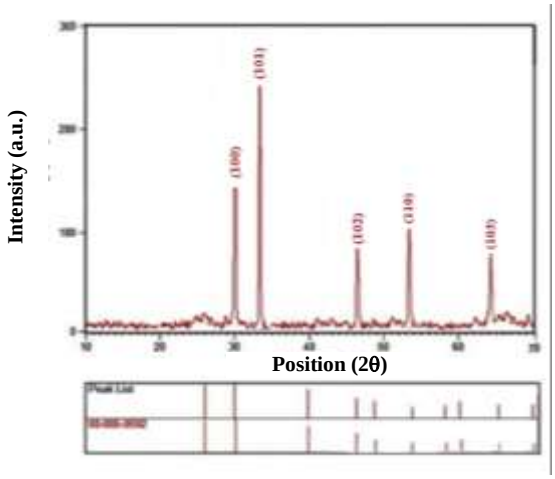

Fig. 3: (a) X-ray diffraction of NiO-SiO_2NPs.

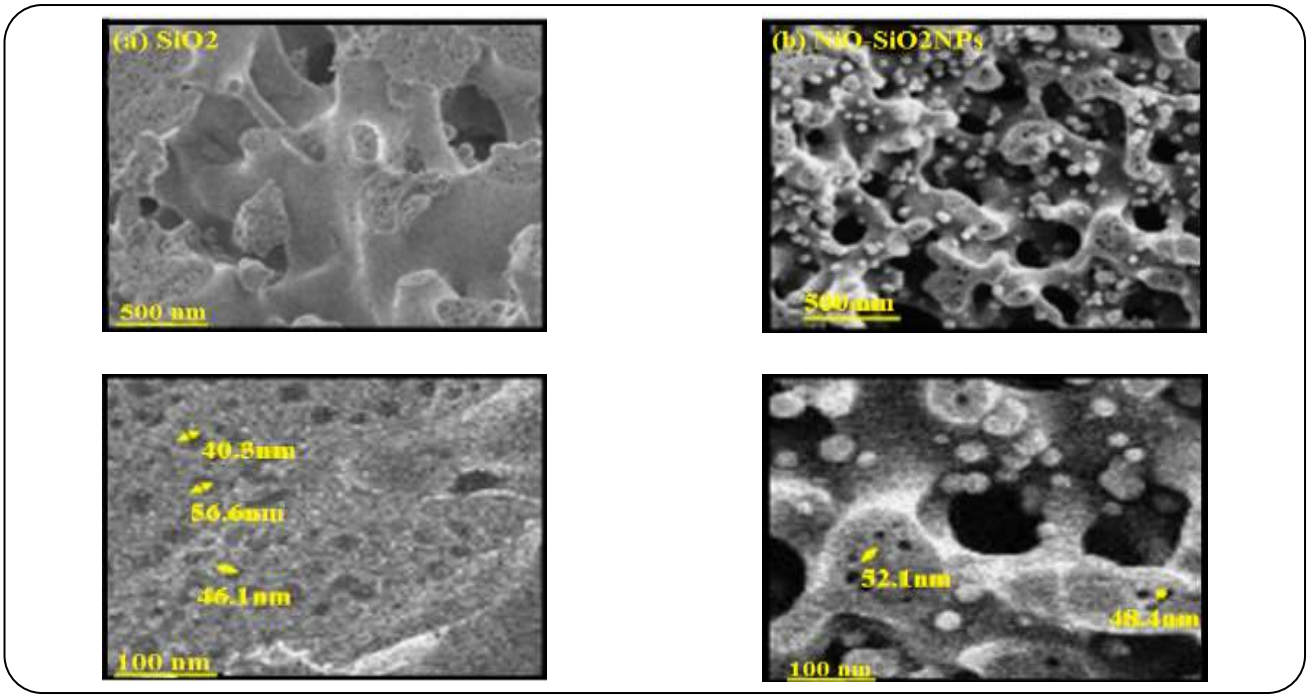

Fig. 4: FE-SEM and energy dispersive X-ray spectra for SiO_2 and NiO-SiO_2NPs.

Surface morphology

The morphological properties of NiO-SiO_2NPs were investigated by FE-SEM and are exhibited in Fig.4 (a,b), the evenness, homogeneity, orderliness, and approximate uniformity of synthesized NiO-SiO_2NPs (even in size distribution) can be observed. NiO-SiO_2NPs after surface modification came to be uneven, bigger, and agglomerate**.** It can be seen that the particles are mostly spherical with various size distributions as they form agglomerates. Based on the particle size distribution, we obtained the average particle size in the range of 40-60 nm very close to those determined by XRD analysis [30, 31]. Fig. 5. The morphology of the macropores is very similar in both the cases. There appears to be fine mesopore structure within the walls of the macropores. The elemental composition of the synthesized monoliths was confirmed by EDS analysis (Fig. 5). Uniform distribution of the precursors throughout the core of the SiO_2 monoliths was responsible for chemical homogeneity.

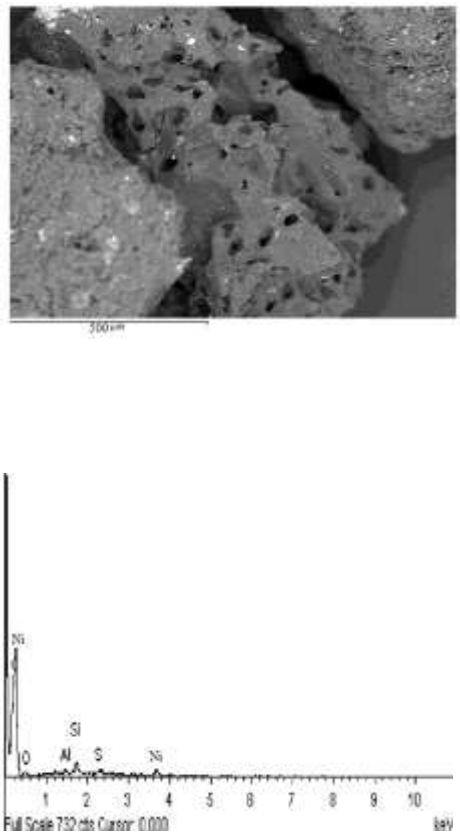

Fig. 5: EDS for SiO_2 and NiO-SiO_2NPs.

Impact of pH on the adsorption

The pH of the adsorbent solution has been identified as one of the most important parameters affecting the removal of the dye. The effect of pH on the MB removal onto SiO_2 and NiO-SiO_2NPs was examined using the batch method.

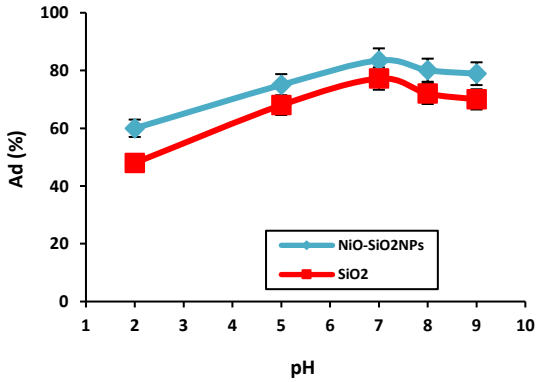

Fig. 6: Impact of initial solution pH on the sorption quantity of MB dye onto SiO_2 and NiO-SiO_2NPs. [MB dye conc = 30 mg/L; adsorbent dose = 0.1g; contact time = 15 min; stirring speed = 180 rpm; temp = 25°C].

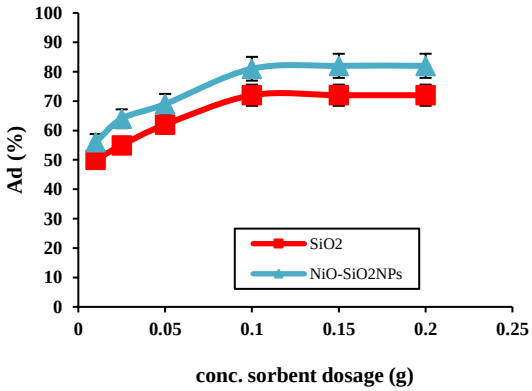

Fig. 7: Impact of dosage SiO_2 and NiO-SiO_2NPs on the adsorption quantity of MB dye. [MB dye conc = 30 mg/L ; pH = 7; contact time = 15 min; stirring speed = 180 rpm; temp = 25°C].

selected pH range was pH 2.0–9.0 (Fig. 6). The maximum adsorption percent was observed at pH 7.0. So remaining all adsorption experiments were carried out at this pH value. The adsorption mechanism may be considered a physicochemical interaction between adsorbent/adsorbate pair [32,33]. At highly acidic pH, the active sites of the adsorbent would be occupied by H^+_{aq} ions, which results in lower uptake of MB dye onto NiO-SiO_2NPs. In turn, the adsorbent surface becomes considerably negatively charged as the pH solution increases from 7.0 to higher values which causes in lower uptake of MB onto SiO_2 and NiO-SiO_2NPs, so the pH =7.0 is the optimum value in the MB adsorption onto the SiO_2 and NiO-SiO_2NPs adsorbent. Previous studies also reported that the maximum absorption efficiency of MB dye on biomass was observed at pH (7.0).

Impact of the dosage of absorbent

The adsorbent dosage is an important parameter because it determines the capacity of an adsorbent for a given initial concentration of the adsorbate. To examine this effect, the experiments were conducted at several doses (0.10 up to 1.10 g). Fig. 7, displays the results. Based on the figure, it may be concluded that dose=0.10 g is a preferred one. The adsorption experiments were done by batch method model. The status of the plot in (fig.7), can explain by the fact that the adsorption sites on the adsorbent surface remain unsaturated at a higher dosage than the optimum dose [34]. When the adsorbent/adsorbate ratio is very small, the available active binding sites are relatively less, so, Ad% becomes low. Therefore, by enhancing the adsorbent/adsorbate ratio, the Ad% increases rapidly and then takes up the gentle changes. This behavior was observed for MB adsorption onto SiO_2 and NiO-SiO_2NPs (see Fig.7).

Impact of the contact time on the adsorption

Since the rate of biosorption is considered crucial for designing batch biosorption experiments, thus, the impact of contact time on the biosorption of (MB) dye by SiO_2 and NiO-SiO_2NPs was examined. A considerable increase in the biosorption of (MB) dye was observed for the contact time of 15 min. The impact of initial dye concentration (MB) dye biosorption by SiO_2 and NiO-SiO_2NPs was scrutinized in batch experiments applying 2 at 25 min contact time, pH value 7 for (MB) dye (30 mg/L), 0.1g adsorbent dose, and the constant temperature 300.15 K. The contact time is an effective factor that affects considerably Ad%. Indeed, for maintaining the adsorbent/adsorbate equilibrium, it should enough prolong the contact time to set up the equilibrium between adsorbent and adsorbate. Fig. 8, shows the effect of contact time on the Ad% for MB adsorption onto SiO_2 and NiO-SiO_2NPs. Based on this figure, the optimum contact time may be chosen as 15.0 min [35].

Impact of the agitation speed

The adsorption process strongly depends on agitation speed owing to the distribution of the solute in the solution and the formation of the external boundary SiO_2 and

NiO-SiO_2NPs. (Fig. 9), demonstrates the removal percent of MB dye (30 mg/L) at different agitation speeds (100–180 rpm) within a contact time of 15 min. From the figure, it is clear that with increasing agitation speed, the percentage removal of dye enhanced from 32.0 to 88.25% for MB dye. The increase in removal percentage can be described by the fact that increasing agitation speed reduces the SiO_2 and NiO-SiO_2NPs boundary layer and surrounding particles, therefore increasing the external SiO_2 and NiO-SiO_2NPs transfer coefficient.

Impact of temperature

To study the effect of temperature on the adsorption percent of MB dye into NiO-SiO_2NPs, the experiments were performed at temperatures range of 298.0 to 348.0 K. Fig.10, shows the results. As can be seen, the Ad% of the process decreases with the temperature increasing. This may come from the fact that the adsorption process may be an exothermic one [36].

Adsorption isotherms

Considering the variation of equilibrium adsorption capacities in terms of the equilibrium concentration (C_e) of the adsorbate, under the optimum values of other parameters, we can examine some suitable isotherms for representing the respect experimental data [37]. To fulfill this goal, we compared the respect experimental results with the three most common isotherm models, including Langmuir, Freundlich, and Temkin isotherms. The nonlinear form of each mentioned model was used for fitting the experimental data in Table 2.

The Langmuir isotherm assumes monolayer adsorption on a homogeneous surface with a restricted number of adsorption sites. Therefore, when a site is occupied, no further sorption can occur at that site. Consequently, the saturation point is equal to the maximum adsorption of the surface. The linearized form of the Langmuir isotherm model is as follows [38]:

$$\frac{C_e}{q_e} = \frac{1}{K_L q_{max}} + \frac{1}{q_{max}} C_e \qquad (3)$$

Where K_L stands for the Langmuir constant associated with the energy of adsorption and q_{max} shows the highest adsorption capacity (mg/g). The calculation of the values of Langmuir parameters (q_{max} and K_L) was done from the slope and discontinuity of the linear plot of Ce/qe versus Ce.

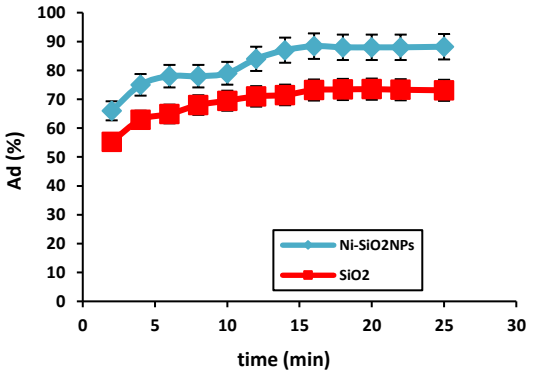

Fig. 8: Impact of contact time on the sorption of MB dye by SiO_2 and NiO-SiO_2NPs. [MB dye conc = 30 mg/L; pH = 7; adsorbent dose = 0.1g; stirring speed = 180 rpm; temp = 25°C].

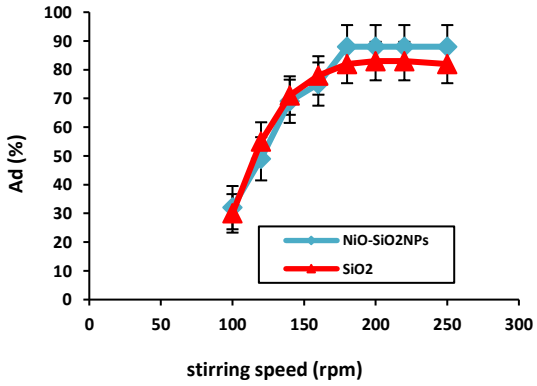

Fig. 9: Impact of contact time on the sorption of MB dye by SiO_2 and NiO-SiO_2NPs. [MB dye conc = 30 mg/L; adsorbent dose = 0.1g; pH = 7; contact time = 15 min; temp = 25°C].

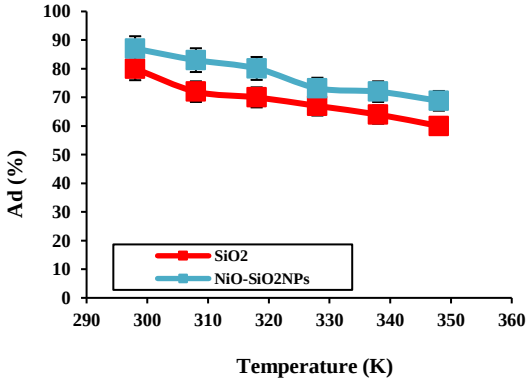

Fig. 10: Impact of temperature on the sorption quantity of MB dye by NiO-SiO_2NPs. [MB dye conc = 30 mg/L; pH = 7; adsorbent dose = 0.1g; time = 15 min; stirring speed = 180 rpm].

The list of values of q_{max}, $K_{L,}$ and regression coefficient R^2 is exhibited in Table 2. Based on the Langmuir model, these values for SiO_2 and NiO-SiO_2NPs sorbent prove the suitability of the sorption phenomena.

2) Freundlich isotherm model is a useful and famous model for defining the adsorption process. This model is based on the assumption that sorption occurs on a non-uniform surface with interactions between adsorbed molecules. Also, the application of the Freundlich equation expresses that sorption energy exponentially lessens with the completion of the sorption sites of an adsorbent. This isotherm is presented as an empirical equation and is applied to explain the non-uniform systems. The linearized form of the equation is as follows [39]:

$$\ln q_e = \ln K_F + \frac{1}{n}\ln C_e \quad (4)$$

In the above formula, K_F stands for the Freundlich constant connected to the bonding energy. *1/n* shows the heterogeneity factor and n (g/L) shows a measure of the deviation from the linearity of adsorption [40]. From the plot of $\ln q_e$ versus lnCe, Freundlich equilibrium constants were found as shown in (Table 2). The degree of non-linearity between solution concentration and adsorption is shown by the n value as follows: if n = 1, then adsorption is linear; if n<1, then adsorption is a physical process; if n>1, then adsorption is a chemical process. As shown in Table 2, the n value in the Freundlich equation was proved to be 2.203 for MB dye by SiO_2 and 1.792 for MB dye by NiO-SiO_2NPs. Therefore, the physical sorption of MB dye onto SiO_2 and NiO-SiO_2NPs is confirmed because n lies between 1 and 10.

3) Temkin isotherm equation. it is presumed that the heat of sorption of all the molecules in the layer reduces linearly with coverage owing to adsorbent–adsorbate interactions and the adsorption is characterized by a homogeneous distribution of the binding energies up to some topmost binding energy [41]. The linear form of the Temkin isotherm is expressed as follows:

$$q_e = B_T \ln K_T + B_T \ln C_e \quad (5)$$

The plots *of ln(C_e)* versus q_e for MB dye are exhibited and in Table 2, the linear isotherm parameters b_T, $K_{T,}$ and the correlation coefficient are summarized. The b_T constant relative to heat of sorption for MB dye onto SiO_2 and NiO-SiO_2NPs adsorbent equals 0.731 J/mol and 0.595 J/mol.

Table 2: Calculated various isotherm constants and related correlation coefficients for the adsorption of the MB dye by SiO_2 and NiO-SiO_2NPs. [MB dye conc = 30 mg/L; adsorbent dose = 0.1 g; pH = 7; contact time = 15 min; stirring speed = 180 rpm; temp = 25°C].

Isotherm	parameters	Value of parameters For NiO-SiO_2NPs	Value of parameters For SiO_2
Langmuir	q_m (mg/g)	140.0	117.0
	K_L (L/mg)	0.418	0.514
	R^2	0.982	0.980
Freundlich	n	1.792	2.203
	K_F $(mg)^{1-n} L^n g^{-1}$	4.198	4.667
	R^2	0.898	0.864
Temkin	B_T (J/mol)	0.595	0.431
	K_T (L/mg)	0.13	0.15
	R^2	0.870	0.841

Further discussion about Langmuir isotherm

Investigation about the adsorption uptake of Methylene Blue (MB) dye was done for an initial concentration range from 5 to 30 mg/L and exhibited in Fig. 11. The essential features of a Langmuir isotherm can be expressed in terms of a dimensionless constant separation factor or equilibrium parameter, R_L that is used to predict if an adsorption system is favorable or unfavorable [42]. Langmuir isotherm can be criticized in terms of a dimensionless constant separation factor or equilibrium parameter, R_L which is used to predict if the isotherm model is favorable or not. The R_L factor is defined as follows:

$$R_L = \frac{1}{1 + K_L C_0} \quad (6)$$

The values of R_L can illustrate the shape of the isotherm to be either unfavorable (R_L>1), linear (R_L=1), favorable (0<R_L<1), or irreversible (R_L=0). The plot of the calculated R_L values versus the initial concentration of MB dye is shown in Fig. 11, indicating that the Langmuir adsorption isotherm is fairly suitable for MB adsorption onto SiO_2 and NiO-SiO_2NPs adsorbent.

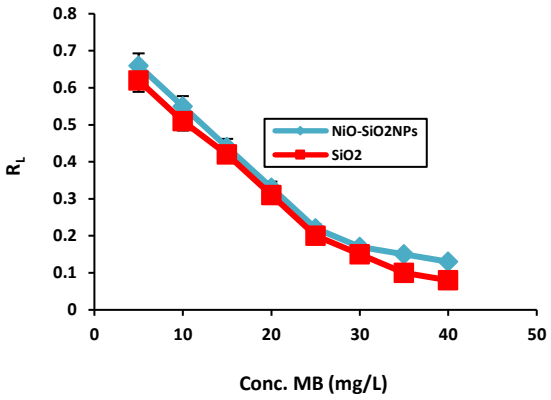

Fig. 11: Plot of R_L versus C_0, that Langmuir isotherm is favorable for representing the experimental data of the MB dye by SiO_2 and NiO-SiO_2NPs. [MB dye conc = 30 mg/L; adsorbent dose = 0.1g; pH = 7; contact time = 15 min; stirring speed = 180 rpm; temp = 25°C].

The adsorption kinetics survey

Adsorption of a solute by a solid in an aqueous solution through complex stages [43], is strongly influenced by several parameters related to the state of the solid (generally with the very heterogeneous reactive surface) and to physic-chemical conditions under which the adsorption occurred. The rate of dye adsorption onto the adsorbent has been fitted to traditional models like pseudo-first-order and pseudo-second-order models and so on. The Lagergren pseudo-first-order model can describe some of the adsorption kinetic data equations and it:

$$\frac{dq_t}{dt} = k_1(q_e - q_t) \quad (7)$$

Where q_e and dq_t (mg/g) are the adsorption capacities at equilibrium and at time t, respectively. k_1 is the rate constant of the pseudo-first-order adsorption (min^{-1}). The integrated form of equation (6) is:

$$\log(q_e - q_t) = \log q_m = \left(\frac{k_1}{2.303}\right)t \quad (8)$$

Thus, the slope of $\log(q_e\text{-}q_t)$ versus t is equal to $\frac{k_1}{2.303}$ and the inception is equal to log q_m [44].

Pseudo-second-order model is represented as:

$$\frac{dq_t}{dt} = k_2(q_e - q_t)^2 \quad (9)$$

$$\frac{t}{q_t} = \frac{1}{k_2 q_e^2} + \frac{t}{q_e} \quad (10)$$

The Intra-particle-diffusion model has based on the hypothesis that the mechanism of dye removal onto a sorbent material occurs through four steps: (1) Bulk diffusion, which is the migration of dye molecules from the bulk solution to the surface of the adsorbent, and (2) Formation the film diffusion, which is the diffusion of dye molecules through the boundary layer to the surface of the adsorbent, and (3) Dye adsorption on the active sites of the surface of the adsorbent, and (4) Intra particle diffusion, which is the migration of dye molecules to the interior pore structure of the adsorbent. The adsorption process is a diffusive mass transfer process where the rate can be expressed in terms of the square root of time (t). The intra-particle-diffusion model can be represented as:

$$q_t = k_i t^{0.5} + I \quad (11)$$

Where k_i is the intraparticle diffusion rate constant (mg/g $min^{0.5}$) and I is the effect of boundary layer thickness. The obtained kinetic data for MB adsorption onto SiO_2 and NiO-SiO_2NPs an adsorbent were examined with the above-mentioned kinetic models. The pseudo-second-order model fitted better the kinetic data of this work more than others (R^2=0.9998, 9982) as shown in (Table 3). [45].

Adsorption thermodynamics

Generally, adsorption thermodynamics is related to the definition of a conditional equilibrium constant (K_c) as:

$$K_c = \frac{q_e}{C_e} \quad (12)$$

Therefore, upon determining K_c at a sufficient number of temperatures, then concluding the thermodynamic functions of the adsorption process is quite straightforward. Because:

$$\Delta G^\circ_{ad} = -RT\ln K_c \quad (13)$$

$$\ln K_c = \frac{\Delta S^\circ_{ad}}{R} - \frac{\Delta H^\circ_{ad}}{RT} \quad (14)$$

$$\ln\left(\frac{K_{c(2)}}{K_{c(1)}}\right) = -\frac{\Delta H^\circ_{ad}}{R}\left(\frac{1}{T_2} - \frac{1}{T_1}\right) \quad (15)$$

Where ΔG^0_{ad}, $\Delta H°_{ad}$ and $\Delta S°_{ad}$ represent respectively the standard change of Gibbs free energy, enthalpy, and entropy associated with the respect adsorption process.

Table 3: The Kinetic parameters for Adsorption of the MB dye by SiO_2 and NiO-SiO_2NPs. [MB dye conc = 30 mg/L; adsorbent dose = 0.1g; pH = 7; contact time = 15 min; stirring speed = 180 rpm; temp = 25°C].

Model	parameters	Value of parameters For NiO-SiO_2NPs	Value of parameters For SiO_2
pseudo-first-order kinetic $\log(q_e - q_t) = \log(q_e) - (\frac{k_1}{2.303})t$	q_m (mg/g)	86.0	72.0
	K_1 (1/min)	0.038	0.03
	R^2	0.9322	0.8373
pseudo-second-order kinetic $t_{/q_t} = \frac{1}{k_2 q_e 2} + \left(\frac{1}{q_e}\right)t$	q_m (mg/g)	144.0	128.0
	K_2(g/mg min)	0.057	0.051
	R^2	0.9998	0.9982
Elovich $q_t = \frac{1}{\beta}ln(\alpha\beta) + \frac{1}{\beta}\ln(t)$	β (mg/g min)	0.0263	0.0414
	α (g/mg)	54.233	75.137
	R^2	0.8459	0.8067

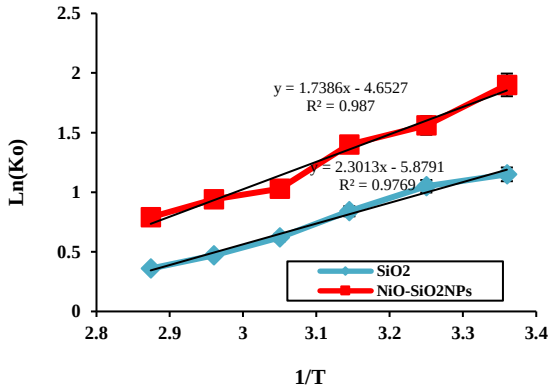

Fig. 12: Plot of ln Kc vs. 1/T for MB dye by SiO_2 and NiO-SiO_2NPs. [MB dye conc = 30 mg/L; adsorbent dose = 0.1g; pH = 7; contact time = 15 min; stirring speed = 180 rpm; temp = 25°C].

T is the temperature in Kelvin. In this research, the values of K_c were calculated at 298.0 at 348.0 K temperatures. The plot of ln K_c versus (1/T) is shown in (Fig. 12), from which the values $\Delta H°_{ad}$ and $\Delta S°_{ad}$ can be deduced (Table 4). As we can see from (Table 4), the values of K_c are greater than 1 at any used temperature, so, $\Delta G°_{ad}$ upon Eq. (13) should be negative indicating that the studied adsorption process is spontaneous in the range of used temperature, $\Delta H°_{ad} < 0$ indicates that the studies adsorption is exothermic. Based on the magnitude of $\Delta H°_{ad}$, we can say that the mentioned adsorption should be physic sorption one and van der Walls interactions are responsible for adsorption taking place. $\Delta S°_{ad} < 0$ indicates a decrease in randomness that occurs during MB dye adsorption onto SiO_2 and NiO-SiO_2NPs, which may come from the MB dye aggregation on the SiO_2 and NiO-SiO_2NPs surfaces [46,47].

Effect of solution Ionic strength

Most dye wastewaters contain salts, and dye adsorption was found to be strongly influenced by the concentration and nature of these ionic species. Since the presence of any ion could affect the hydrophobic and electrostatic interactions between dyes and the surface of SiO_2 and NiO-SiO_2NPs as an adsorbent, the effect of solution ionic strength on the removal of MB dye was investigated under the optimum experimental conditions in batch technique (Table 5). Selected concentrations of NaCl, in the range of (0.01-1.0 M), were added to individual beakers containing 50 mL of the tested MB dye solution (30 mg/L). The solution pH and SiO_2 and NiO-SiO_2NPs dosage were fixed at 7.0 and 0.1g, respectively, and the stirring time was 15 min. After the mixing time elapsed, the SiO_2 and Ni-SiO_2NPs were magnetically separated and the solution was analyzed for the residual dyes. The results indicated that the adsorption SiO_2 and NiO-SiO_2NPs for MB dye were not significantly affected by increasing NaCl concentration. This indicates that Na^+ and Cl^- ions do not compete with the positively or negatively charged groups of the MB dye molecules for being adsorbed onto SiO_2 and NiO-SiO_2NPs.

Recycling of the adsorbent

The ability to recover and reusing of the adsorbent was tested in several steps of adsorption and the desorption process were done [48]. The results are shown in (Fig.13).

Table 4: The thermodynamic parameters of MB dye adsorption onto SiO_2 and NiO-SiO_2NPs. [MB dye conc = 30 mg/L; adsorbent dose = 0.1g; pH = 7; contact time = 15 min; stirring speed = 180 rpm; temp = 25°C].

MB dye (30mg/L)	T (^{O}K)	K_d	Value of ΔG^o(kJ/mol)	Value of ΔH^o (kJ/mol)	Value of ΔS^o (kJ/mol K)
Sorbent NiO-SiO_2NPs	298	3.17	-2.858	-14.455	-38.683
	308	2.76	-2.6		
	318	2.33	-2.236		
	328	1.87	-1.706		
	338	1.62	-1.356		
	348	1.43	-1.035		
Sorbent SiO_2	298	8.09	-5.18	-21.65	-56.4
	308	4.88	-4.06		
	318	3.55	-3.35		
	328	3.27	-3.24		
	338	2.57	-2.653		
	348	2.13	-2.188		

Table 5: Effect of the Ionic Strength on the removal of the MB dye by SiO_2 and NiO-SiO_2NPs. [MB dye conc = 30 mg/L; adsorbent dose = 0.1g; pH = 7; contact time = 15 min; stirring speed = 180 rpm; temp = 25°C].

NaCL (M)	Value of parameters For NiO-SiO_2NPs	Value of parameters For SiO_2
0.00	81.7	78.2
0.02	82.2	78.1
0.04	82.04	78.15
0.06	82.0	78.12
0.08	81.5	78.06
0.1	82.6	78.16
0.2	82.1	78.2
0.4	81.9	78.15
0.6	81.6	78.10
0.8	82.2	78.07
1.0	82.4	78.12

As shown in the figure 88.2% of MB dye was desorbed in the first run and after 6 runs, there were slight changes in MB dye desorption. So, it was concluded that the desired removal of 88.2% can be achieved after 6 runs.

Comparison of MB dye onto sorbent adsorption method with other

A comparison of the maximum adsorption capacities of different adsorbents for the removal of MB dye was also reported in (Table 6). The type and density of active sites in adsorbents which are responsible for the adsorption of MB dye from the solution result in the variation in q_{max} values. The outcomes of the table clearly show that the sorption capacity of the utilized sorbent in the current study is significantly high. In general, the morphology, particle size and distribution, and surface structure of this sorbent were effective in its successful outcomes.

Table 6: Comparison of the adsorption capacities of different adsorbents for the adsorption of MB dye with other sorbent.

Dye	sorbent	Dosage sorbent (g)	Adsorption capacity (mg/g)	References
MB dye	Coconut (Cocos nucifera) shell with (H_2SO_4)	0.2	50.6	[3]
MB dye	activated carbon (AC) *via* H_3PO_4	1.0	241.3	[8]
MB dye	CS-MgONP	0.47	19.37	[12]
MB dye	MgONP-AC	0.47	78.7	[13]
MB dye	Mn-doped PbS NPs	0.025	200.0	[15]
MB dye	(3-AS), (3-APTMS) and (3-MPTMS)	0.1	4.95, 5.20 and 5.31	[21]
MB dye	S-CS-MT	1.5	188.2	[24]
MB dye	Zr-SBA-15	0.066	310.88	[39]
MB dye	walnut carbon	0.225	4.716	[46]
MB dye	***S***iO_2 and NiO-SiO_2NPs	0.1	140.0 and 117.0	Present study

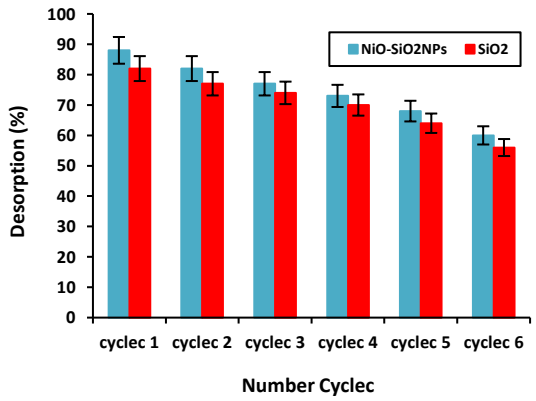

Fig. 13: Desorption of the MB dye by SiO_2 and NiO-SiO_2NPs. [MB dye conc = 30 mg/L; adsorbent dose = 0.1g; pH = 7; contact time = 15 min; stirring speed = 180 rpm; temp = 25°C].

CONCLUSIONS

Synthesized NiO-SiO_2NPs and their characterization revealed that the synthesized adsorbent has a good ability for MB removal from aqueous media. Using this synthesized adsorbent various experiments were done to evaluate the effect of pH, adsorbent dosage (dose), initial MB dye concentration (C_0) contact time (tc), and temperature (T) on the removal percentage (Ad%) of MB dye onto NiO-SiO_2NPs were studied and the optimum value of each factor was determined (pH=7, dose=0.1g, C_0=30 mg/L, tc=15 min, and T=298.0 K). So, as a result, we reached to Ad%=% 88.2 at optimum conditions. In general, the effect of pH on Ad% is more important than other effects, because solution pH seriously the physicochemical properties of adsorbent and adsorbate, and H_{aq}^+ and OH_{aq}^- come into conception with the main adsorbate at low and high pH receptively. The experimental equilibrium data were fitted to the conventional isotherm models and accordingly, Langmuir isotherm has good applicability for the explanation of experimental data with maximum adsorption capacity of the MB dye for SiO_2 and NiO-SiO_2NPs were roughly 117.0 and 140.0 mg/g respectively. Three kinetics equations were used to evaluate, the kinetic behavior of the studied adsorption process. This revealed that the kinetic data of this research is well fitted pseudo-second-order equation (R^2=0.9998 and 0.9982). The thermodynamic analysis was considered by introducing a conditional equilibrium constant (K_c) by which estimating the thermodynamic parameters of the adsorption process becomes a possibility. The Van's Hoff plot of lnK_c versus (1/T) was satisfactorily linear. This result allowed us to estimate $\Delta H°_{ad}$ and $\Delta S°_{ad}$ from the slope and intercept of the plot respectively. $\Delta G°_{ad}$ was calculated on the basis of $\Delta H°_{ad}$ and $\Delta S°_{ad}$ or directly from K_c at each experimental temperature. The MB adsorption onto NiO-SiO_2NPs was spontaneous ($\Delta G°_{ad}$ <0) and exothermic ($\Delta H°_{ad}$ <0), but with a decrease in randomness ($\Delta S°_{ad}$<0). Regarding the magnitude of $\Delta H°_{ad}$, we concluded that the studied adsorption in this work is physical adsorption. As a final result, we should claim that the synthesized SiO_2 and NiO-SiO_2NPs have a good capacity for removing MB dye

and the other dyes from aqueous media as a low-cost, available, and efficient adsorbent.

Acknowledgment

The authors gratefully acknowledge the support of this work by Islamic Azad University, Omidiyeh Branch, Omidiyeh, Iran, for their partial support of this work.

Received : May. 16, 2021 ; Accepted : Aug. 16, 2021

REFERENCES

[1] Marahel F., Adsorption of Hazardous Methylene Green Dye from Aqueous Solution onto Tin Sulfide Nanoparticles Loaded Activated Carbon: Isotherm and Kinetics Study, *Iran. J. Chem. Chem. Eng. (IJCCE),* **38(5)**: 129-142 (2019).

[2] Senthilkumar R., Reddy Prasad D.M., Govindarajan L., Saravanakumar K., Naveen Prasad B.S., Improved Sorption of Reactive Black 5 by Date Seed-Derived Biochar: Isotherm, Kinetic, and Thermodynamic Studies, *Separa. Sci. Technol.*, **54(15)**: 2351-2360 (2019).

[3] Jawad A.H., Abdulhameed A.S., Mastuli M.S., Acid-Factionalized Biomass Material for Methylene Blue Dye Removal: A Comprehensive Adsorption and Mechanism Study, *J. Taibah, Univ. Sci.*, **14(1)**: 305–313 (2020).

[4] Jawad A.H., Abdulhameed A.S., Statistical Modeling of Methylene Blue Dye Adsorption by High Surface Area Mesoporous Activated Carbon from Bamboo Chip Using KOH-Assisted Thermal Activation, *Energ. Ecol. Environ.*, **5(5)**: 1-17 (2020).

[5] Azari A., Nabizadeh R., Nasseri S., Mahvi A.H., Mesdaghinia A.R., Comprehensive Systematic Review and Meta-Analysis of Dyes Adsorption by Carbon-Based Adsorbent Materials: Classification and Analysis of Last Decade Studies, *Chemosphere*., **250**: 126238- 126246 (2020).

[6] Ramezani F., Zare-Dorabei R., J. Simultaneous Ultrasonic-Assisted Removal of Malachite Green and Methylene Blue from Aqueous Solution by Zr-SBA-15, *Polyhedron.*, **166**: 153-162 (2019).

[7] Daraei H., Mittal A., Investigation of Adsorption Performance of Activated Carbon Prepared from Waste Tire for the Removal of Methylene Blue Dye from Wastewater, *J. Desal. Water. Treat.*, **90**: 294–298 (2017).

[8] Jawad A.H., Firdaus Hum N.N.M., Abdulhameed A.S., Mohd Ishak M.Z., Mesoporous Activated Carbon from Grass Waste Via H_3PO_4-Activation for Methylene Blue Dye Removal: Modelling, Optimisation, and Mechanism Study, *Int. J. Environ. Anal. Chem.*, **99**: 1-20 (2020).

[9] Jawad A.H., Abdulhameed A.S., Surip S.V., Sabar S., Adsorptive Performance of Carbon Modified Chitosan Biopolymer for Cationic Dye Removal: Kinetic, Isotherm, Thermodynamic, and Mechanism Study, *Int. J. Environ. Anal. Chem.*, **99**: 1-18 (2020).

[10] Abdulhameed A.S., Firdaus Hum N.N.M., Rangabhashiyam S., Jawad A.H., Wilson L.D., Yaseen Z.M., Al-Kahtani A.A., ALOthman Z.A., Statistical Modeling and Mechanistic Pathway for Methylene Blue Dye Removal by High Surface Area and Mesoporous Grass-Based Activated Carbon Using K_2CO_3 Activator, *J. Environ. Chem. Eng.*, **9**: 105530(2021).

[11] Saravanakumar K., Naveen Prasad B.S., Senthilkumar R., Manickam S., Reddy Prasad D.M., Gajendiran V., Batch and Column Arsenate Sorption Using Turbinaria ornata Seaweed Derived Biochar: Experimental Studies and Mathematical Modeling, *Chemistry Select.*, **5**: 3661-3668 (2020).

[12] Venkata Ratnam M., Nagamalleswara Rao K., Meena V., Methylene Blue Adsorption by Magnesium Oxide Nanoparticles Immobilized with Chitosan (CS-MgONP): Response Surface Methodology, Isotherm, Kinetics and Thermodynamic Studies, *Iran. J. Chem. Chem. Eng. (IJCCE),* **39(6)**: 29-42 (2020).

[13] Venkata Ratnam M., Punugoti T., Sasi Kala N., Kanidarapu N.R., Meena V., Modelling and Optimization of Methylene Blue Adsorption onto Magnesium Oxide Nanoparticles loaded onto Activated Carbon (MgONP-AC): Response Surface Methodology and Artificial Neural Networks, *Materials. Today. Proceedings.*, **18**: 4932–4941 (2019).

[14] Venkata Ratnam M., Karthikeyan C., Nagamalleswara Rao K., Meena, V., Magnesium Oxide Nanoparticles for Effective Photocatalytic Degradation of Methyl Red Dye in Aqueous Solutions: Optimization Studies Using Response Surface Methodology, *Materials. Today. Proceedings.*, **26(2)**: 2308-2313 (2020).

[15] Marahel F., Mombini Godajdar B., Niknam L., Faridnia M., Pournamdari E., Mohammad Doost, S., Ultrasonic Assisted Adsorption of Methylene Blue Dye and Neural Network Model for Adsorption of Methylene Blue Dye by Synthesized Mn-doped PbS Nanoparticles, *Int. J. Environ. Anal. Chem.*, **101(5)**: 1-22 (2021).

[16] Reghioua A., Barkat D., Jawad A.H., Abdulhameed A.S., Al-Kahtani A.A., ALOthman Z.A., Parametric Optimization by Box–Behnken Design for Synthesis of Magnetic Chitosan-Benzil/ZnO/Fe_3O_4 Nanocomposite and Textile Dye Removal, *J. Environ. Chem. Eng.*, **9**: 105166 (2021).

[17] Reghioua A., Barkat D., Jawad A.H., Abdulhameed A.S., Khan M.R., Synthesis of Schiff's Base Magnetic Crosslinked Chitosan-Glyoxal/ZnO/Fe_3O_4 Nanoparticles for Enhanced Adsorption of Organic Dye: Modeling and Mechanism Study, *Sustaina. Chem. Pharmac.*, **20**: 100379 (2021).

[18] Nourozi S., Zare-Dorabei R., Highly Efficient Ultrasonic-Assisted Removal of Methylene Blue from Aqueous Media By Magnetic Mesoporous Silica: Experimental Design Methodology, Kinetic and Equilibrium Studies, *J. Desal. Water. Treat.*, **85**: 184-196 (2017).

[19] Senthilkumar R., Reddy Prasad D.M., Govindarajan L., Saravanakumar K., Naveen Prasad B.S., Synthesis of Green Marine Algal-Based Biochar for Remediation of Arsenic(V) From Contaminated Waters in Batch and Column Mode of Operation, *Int. J. Phytoremedia.*, **22(3)**: 1-18 (2019).

[20] Zhao G., Zhao Q., Jin X., Wang H., Zhang K., Li M., Wang N., Zhao W., Meng S., Mu R., Preparation of a Novel Hafnium-Loaded Fe_3O_4@SiO_2 Superparamagnetic Nanoparticles and its Adsorption Performance for Phosphate in Water, *J. Desal. Water. Treat.*, **216**: 188-198 (2021).

[21] Sogut E.G., Ergan E., Cilic N.C., Donmaz H., Methylene Blue Adsorption from Aqueous Solution by Functionalized Perlites: An Experimental and Computational Chemistry Study, *J. Desal. Water. Treat.*, **217**: 391-410 (2021).

[22] Naushad Mu., Sharma G., Alothman A., Photodegradation of Toxic Dye Using Gum Arabic-Crosslinkedpoly (acrylamide) / $Ni(OH)_2$ / FeOOH Nanocomposites Hydrogel. *J. Clean. Production.*, **241**: 112863 (2019).

[23] Arora C., Soni S., Sahu S., Mittal J., Kumar P., Bajpai P.K., Iron Based Metal Organic Framework for Efficient Removal of Methylene Blue Dye from Industrial Waste, *J. Molecular. Liquids.*, **284**: 373-352 (2019).

[24] Abdul Mubarak N.S., Bahrudin N.N., Jawad A.H., Hameed B.H., Sabar S., Microwave Enhanced Synthesis of Sulfonated Chitosan-Montmorillonite for Effective Removal of Methylene Blue, *J. Polymers. Environment*, **29(12)**: 4027- 4039 (2021).

[25] Liu J., Peng Z.Y., Huang H.W., Li Y., Wu M., Ke X.X., Tendeloo G.V., Su B.L., 2D ZnO Mesoporous Single-Crystal Nanosheets With 0001 Polar Facets for the Depollution of Cationic Dye Molecules by Highly Selective Adsorption and Photocatalytic Decomposition, *J. Appl. Catal. B: Environ.*, **181**: 138-145 (2016).

[27] Tang R., Dai C., Li C., Liu W., Gao S., Wang C., Removal of Methylene Blue from Aqueous Solution Using Agricultural Residue Walnut Shell: Equilibrium, Kinetic, and Thermodynamic Studies, *J. Chemistry.*, **10**: 1155-1165 (2017).

[28] Auta M., Hameed B.H., Chitosan-Clay Composite as Highly Effective and Low-Cost Adsorbent for batch and Fixed-Bed Adsorption of Methylene Blue, *J. Chem. Engineering.*, **237**: 350-361 (2014).

[29] Feng J., Wang Y., Zou L., Li B., He X., Ren Y., Lv Y., Fan Z., Synthesis of Magnetic Zno/$ZnFe_2O_4$ by a Microwave Combustion Method and its high Rate of Adsorption of Methylene Blue, *J. Colloid. Interf. Sci.*, **438**: 318-322 (2015).

[30] Malek N.N.A., Jawad A.H., Abdulhameed A.S., New Magnetic Schiff's Base-Chitosan-Glyoxal/Fly Ash/Fe_3O_4 Biocomposite for the Removal of Anionic Azo Dye: An Optimized Process, *Int. J. Biolog. Macromole.*, **146**: 530-539 (2020).

[31] You K.E., Park J.H., Kim Y.C., Oh S.G., Magnetic Properties and Dye Adsorption Capacities of Silica - Hematite Nanocomposites with Well - Defined Structures Prepared in Surfactant Solutions, *J. Solid. State. Sci.*, **33**: 38-44 (2014).

[32] Hajati S., Ghaedi M., Mazaheri H., Removal of Methylene Blue from Aqueous Solution by Walnut Carbon: Optimization Using Response Surface Methodology, *J. Desal. Water. Treat.*, **57**: 3179-3193 (2016).

[33] Zare Khafri H., Ghaedi M., Asfaram A., Safarpoor M., Synthesis and Characterization of ZnS:Ni-NPs Loaded on AC Derived from Apple Tree Wood and their Applicability for the Ultrasound Assisted Comparative Adsorption of Cationic Dyes Based on the Experimental Design, *Ultrason Sonochem.*, **38**: 371 (2017).

[34] Wei W., Yang L., Zhong W.H., Li S.Y., Cui J., Wei Z.G., Fast Removal of Methylene Blue from Aqueous Solution by Adsorption onto Poorly Crystalline Hydroxyapatite Nanoparticles, *Nanomaterials and Biostructures.*, **10**: 1343-1363 (2015).

[35] Xiao N., Adsorptive Removal and Kinetics of Methylene Blue from Aqueous Solution Using NiO/MCM-41 composite, Phys. E: Low-Dimens, *Syst. Nanostruct.*, **65**: 4-12 (2015).

[36] Ali L., Zhang C., Chen Z., Removal of Methylene Blue from Aqueous Solution by a Solvothermal-Synthesized Graphene/Magnetite Composite, *J. Hazard. Mater.*, **192**: 1515–1524 (2011).

[37] Pathania D., Sharma S., Singh P., Removal of Methylene Blue by Adsorption onto Activated Carbon Developed from Ficus Carica Bast, *Arab. J. Chem.*, **10**: 1445–1451 (2017).

[38] Yang Y., Xie Y., Pang L., Li M., Song X., Wen J., Zhao H., Preparation of Reduced Graphene Oxide/Poly(Acrylamide) Nanocomposite and Its Adsorption of Pb^{2+} And Methylene Blue, *Langmuir.*, **29**: 10727-10736 (2013).

[39] Dehghani M.H., Dehghan A., Alidadi H., Dolatabadi M., Mehrabpour M., Converti A., Removal of Methylene Blue Dye from Aqueous Solutions by a New Chitosan/Zeolite Composite from Shrimp Waste: Kinetic and Equilibrium Study, *Korean. J. Chem. Eng.*, **34(6)**: 1699-1707 (2017).

[40] Mahini R., Esmaeili H., Foroutan R., Adsorption of Methyl Violet from Aqueous Solution Using Brown Algae Padina Sanctae-Crucis, *Turk. J. Biochem.*, **24**: 1-12 (2018).

[41] Zubair M., Ihsanullah I., Jarrah N., Khalid A., Manzar M.S., Kazeem T.S., Al- Harthi M.A., Starch-NiFe-Layered Double Hydroxide Composites: Efficient Removal of Methyl Orange from Aqueous Phase, *J. Molecular. Liquids.*, **249**: 254–264 (2018).

[42] Fu J., Chen Z., Wang M., Liu S., Zhang J., Han R., Xu Q., Adsorption of Methylene Blue by a High-Efficiency Adsorbent (Polydopamine Microspheres): Kinetics, Isotherm, Thermodynamics and Mechanism Analysis, *Chem. Eng. J.*, **259**: 53-61 (2015).

[43] Ghaedi M., Heidarpour S., Nasiri S., Kokhdan S., Daneshfar A., Brazesh B., Comparison of Silver and Palladium Nanoparticles Loaded on Activated Carbon for Efficient Removal of Methylene Blue: Kinetic and Isotherm Study of Removal Process, *J. Powder. Technol.*, **228**: 18-25 (2012).

[44] Toor M., Jin B., Adsorption Characteristics, Isotherm, Kinetics, and Diffusion of Modified Natural Bentonite for Removing Diazo Dye, *J. Chem. Eng.*, **187**: 79-88 (2012).

[45] Aarfane A., Salhi A., El Krati M., Tahiri S., Monkade M., Lhadi E.K., Bensitel M., Kinetic and Thermodynamic Study of the Adsorption of Red195 and Methylene Blue Dyes on Fly Ash and Bottom Ash in Aqueous Medium, *J. Mater. Environ. Sci.*, **5**: 1927-1939 (2014).

[46] Hajati S., Ghaedi M., Barazesh B., Karimi F., Sahraei R., Daneshfar A., Asghari A., Application of High Order Derivative Spectrophotometry to Resolve the Spectra Overlap Between BG and MB for the Simultaneous Determination of Them: Ruthenium Nanoparticle Loaded Activated Carbon as Adsorbent, *J. Ind. Eng. Chem.*, **20**: 2421–2427 (2014).

[47] Yagub M.T., Sen T.K., Ang H.M., Equilibrium, Kinetics, and Thermodynamics of Methylene Blue Adsorption by Pine Tree Leaves, *J. Water. Air. Soil. Pollut.*, **223**: 5267–5282 (2012).

[48] Sabri A.A., Albayati T.M., Alazawi R.A., Synthesis of Ordered Mesoporous SBA-15 and Its Adsorption of Methylene Blue, *Korean. J. Chem. Eng.*, **32(9)**: 1835-1841 (2015).